

pubs.acs.org/JACS Article

Accelerated Prediction of Phase Behavior for Block Copolymer Libraries Using a Molecularly Informed Field Theory

Charles Li, Elizabeth A. Murphy, Stephen J. Skala, Kris T. Delaney, Craig J. Hawker,* M. Scott Shell,* and Glenn H. Fredrickson*



Cite This: https://doi.org/10.1021/jacs.4c11258



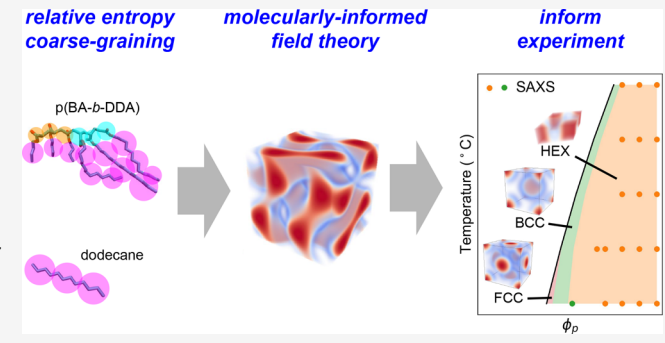
ACCESS I

Metrics & More

Article Recommendations

sı Supporting Information

ABSTRACT: Solution formulations involving polymers are the basis for a wide range of products spanning consumer care, therapeutics, lubricants, adhesives, and coatings. These multicomponent systems typically show rich self-assembly and phase behavior that are sensitive to even small changes in chemistry and composition. Longstanding computational efforts have sought techniques for predictive modeling of formulation structure and thermodynamics without experimental guidance, but the challenges of addressing the long time scales and large length scales of self-assembly while maintaining chemical specificity have thwarted the emergence of general approaches. As a consequence, current formulation design remains largely Edisonian. Here, we present a



multiscale modeling approach that accurately predicts, without any experimental input, the complete temperature—concentration phase diagram of model diblock polymers in solution, as established postprediction through small-angle X-ray scattering. The methodology employs a strategy whereby atomistic molecular dynamics simulations is used to parametrize coarse-grained field-theoretic models; simulations of the latter then easily surmount long equilibration time scales and enable rigorous determination of solution structures and phase behavior. This systematic and predictive approach, accelerated by access to well-defined block copolymers, has the potential to expedite *in silico* screening of novel formulations to significantly reduce trial-and-error experimental design and to guide selection of components and compositions across a vast range of applications.

■ INTRODUCTION

An enormous range of products in everyday life-spanning detergents, paints, personal care products, and lubricants-are complex formulations that contain a variety of solvents, small molecules, surfactants, and polymers. These mixtures can phase separate and self-assemble into a variety of structures that greatly influence the properties and hence performance of the formulation. 1-10 For example, the salt concentration in shampoos and shower gels is carefully tuned to trigger the selfassembly of surfactants into wormlike micelles, which entangle and produce an increase in viscoelasticity that gives these products their characteristic gel-like consistency.² However, the large number of components in such formulations and the breadth of ingredients that can be incorporated leads to an extensive design space, which makes it difficult to optimize such products via costly and laborious trial-and-error methods. 11,12 Furthermore, traditional design approaches are enabled by extensive background knowledge and heuristics developed over decades of experience; such prior expertise becomes largely irrelevant as industry looks toward new sustainable and biobased formulation components and building blocks, for which little accrued knowledge and characterization exists. 13-18

To enable the next generation of formulated products, more effective and systematic screening approaches are needed to reduce development time and costs. Computational modeling approaches have long been an attractive target for guiding experimental efforts and augment existing formulation design efforts in industry, but current methods fall short of broadly capable *in silico* screening platforms. For example, atomistic simulations are widely used in research and industry and have been used to model a variety of phenomena relevant to formulation design such as self-assembly in surfactant solutions, 20,21 temperature-induced conformational changes in lubricant viscosity modifiers, 22,23 and drug solubility. However, their high computational cost limits the ability to simulate high-molecular weight polymers and to reach the time scales necessary for capturing self-assembly on mesoscopic (10 nm $-10~\mu$ m) length scales, which are critical features of many

Received: August 15, 2024 Revised: October 9, 2024 Accepted: October 10, 2024



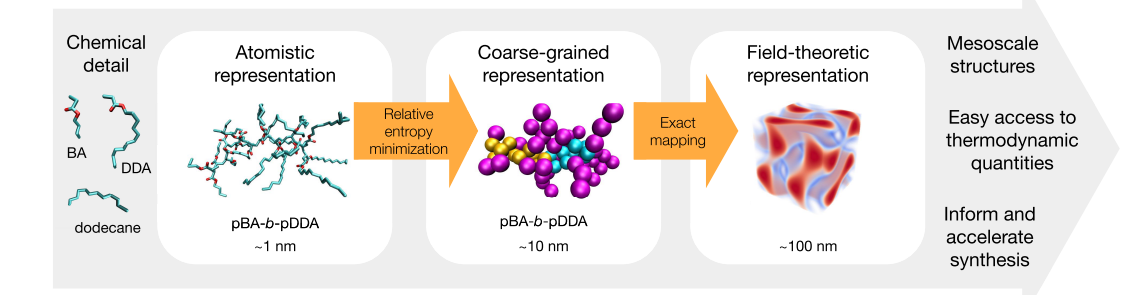


Figure 1. Small-scale, atomistic molecular dynamics (MD) simulations are conducted of a low molecular weight polymeric solution with the monomer chemistries of interest. Here, we consider a model system consisting of poly(butyl acrylate)-block-poly(dodecyl acrylate) (pBA-b-pDDA) in a dodecane solvent. The all-atom results are then systematically transformed into CG particle models by relative entropy minimization, which determines the optimal effective coarse interactions. The CG particle models are subsequently analytically converted to a statistical field theory and simulated at realistic molecular weights using field-theoretic methods.

complex solution formulations. Additionally, free energies and chemical potentials are difficult to access in particle-based simulations as they require specialized, computationally expensive techniques that become intractable for species of any modest molecular weight. This makes it challenging if not impossible to establish equilibrium phase behavior and map phase diagrams across formulation conditions of interest.

To address these issues, many efforts have used coarsegrained (CG) models that map atomistic models to coarser "bead" representations, sacrificing chemical detail for modest gains in computational efficiency. 26-35 For example, a type of mesoscopic CG approach called dissipative particle dynamics (DPD), which employs momentum-conserving dissipative forces, 36-39 is widely used in industry to model complex polymer and surfactant solutions relevant to formulation design. 40,41 However, DPD models used for these purposes are typically ad hoc with no clear connection to underlying chemical details, limiting their ability for predictive modeling of novel components. 42 Moreover, while enabling larger-scale simulations, DPD and other CG particle models still suffer the same drawbacks as their more-detailed atomistic counterparts, struggling to access spatiotemporal scales associated with realistic polymeric formulations, and requiring complex and expensive techniques for assessing phase stability and constructing phase diagrams. For example, time scales for micelle formation in diblock copolymer solutions or mesophase transformations can be on the order of hours or longer, 43 which far exceeds the capabilities of CG molecular dynamics.

Here, we propose an alternative, general formulation modeling approach that is directly predictive of equilibrium structures and phase diagrams, computationally efficient, and readily suited to large-scale simulations. Specifically, we exploit equilibrium field-theoretic simulation methods that efficiently simulate high molecular weight polymers while capturing structural features on mesoscopic length scales. 44-46 Fieldtheoretic methods recast CG particle models as statistical field theories involving auxiliary potential fields, avoiding the computational cost of tracking explicit particle coordinates. This effectively decouples pairwise intermolecular interactions into particle-field interactions, and in turn enables rapid equilibration through field-based sampling methods, even for complex, large-scale self-assembling systems.⁴⁷ Moreover, field theories provide direct access to critical thermodynamic quantities, such as chemical potentials and free energies,

which when combined with efficient variable cell shape techniques, ⁴⁸ allow for rigorous determination of the stable (i.e., most favorable) structures and phases at equilibrium. ⁴⁹ Field-theoretic approaches have historically relied on experimentally determined parameters – in particular, Flory–Huggins χ -parameters ⁵⁰ – to describe interactions between polymer and solvent species. However, these interaction parameters are challenging to measure experimentally, ⁵¹ and the need for such experimental input has proved limiting in the application of field-theoretic simulations to new systems and for enabling mesoscopic *in silico* screening.

In this work, we exploit a bottom-up, predictive approach for modeling polymer solution phase behavior that leverages the significant advantages of field-theoretic methods in reaching large scales while retaining the chemical accuracy of atomistically resolved molecular dynamics models by using a multiscale approach to determine field-theoretic interactions from the bottom-up. This approach utilizes small-scale atomistic simulations to initially parametrize CG particle models, which are then analytically transformed into a field-theoretic representation, thereby embedding chemical specificity and providing access to a broad range of structural and thermodynamic properties by field theoretic simulations. 52-55 We then couple this strategy with advanced synthesis techniques for preparing well-defined macromolecules with accurate control over molecular weight, dispersity, and block lengths. We demonstrate the power of this workflow by making de novo predictions of temperature and concentration-dependent phase behavior for binary mixtures of poly(butyl acrylate)block-poly(dodecyl acrylate) (pBA-b-pDDA) copolymers in dodecane solvent. Here we choose acrylic block copolymers as a model system because they are synthetically highly tunable and exhibit a broad range of phase behaviors. 56,57 The predicted, complex phase behavior shows remarkably good agreement with small-angle X-ray scattering (SAXS) analysis of solutions prepared from model pBA-b-pDDA copolymers synthesized using photoinduced atom transfer radical polymerization (photo-ATRP). The ability to predictively capture the mesoscale structure and phase behavior of complex, selfassembling systems without preexisting experimental data demonstrates the potential of this combined multiscale modeling and synthesis approach to greatly accelerate the discovery of novel formulations.

RESULTS AND DISCUSSION

Molecularly Informed Field Theory. By using atomistic models to inform interaction parameters, field-theoretic simulations no longer rely on experimental parameters, enabling a rigorous and predictive determination of equilibrium mesoscale properties connected to the underlying chemistry (Figure 1). CG particle models serve as the crucial link in this connection, where representative atomistic simulations of a system of interest are mapped into a coarser particle representation using a systematic coarse-graining technique called relative entropy (S_{rel}) minimization; this step seeks to minimize information loss when transitioning to the coarser representation. 58,59 The S_{rel} minimization approach has been used to develop and study CG models of a wide variety of biological and soft matter systems including peptides, ^{60,61} proteins, ^{62,63} liquid mixtures, ⁶⁴ and surfactants. ⁵⁸ Further details on S_{rel} minimization coarse graining are found in Section S2 in the Supporting Information. Here, we map our reference systems to CG models that feature soft pairwise Gaussian nonbonded interactions and intramolecular harmonic bonds. The nonbonded interactions in the resulting CG models facilitate an exact analytical transformation to a fieldtheoretic representation by using Hubbard-Stratonovich transforms. 44,65,66 While the CG particle and field-theoretic representations are equivalent, the mathematical structure of the field theory allows straightforward access to chemical potentials and free energies, 49 enabling phase coexistence calculations and construction of phase diagrams, tasks that are tedious and computationally expensive to perform with particle-based simulation methods. Additionally, the fieldtheoretic representation allows for equilibration and sampling of systems at speeds that are orders of magnitude faster than particle-based methods and nearly independent of system density.46,47

The present study is the first to employ this computational framework to establish a predictive workflow to guide experimental synthesis of novel polymeric formulations. While earlier studies from our group demonstrated the ability of this modeling approach to anticipate experimental results, ^{52–54} they were limited to systems that were already characterized. Here, the synergistic interaction with synthesis and experiment first develops this modeling framework as a mechanism to accelerate materials discovery by targeting only the most promising formulations for laboratory realization.

Informing Copolymer Synthesis Using Spinodal Calculations. Our model system consists of a pBA-b-pDDA copolymer in a dodecane solvent (Figure 2a), and we target a moderate total degree of polymerization, N, of 150 with accurate control over block length. Following the methodology discussed above, we develop a field-theoretic representation of the system in the following manner. We first perform atomistic simulations of the dodecane solvent and solutions containing pBA and pDDA oligomers 25 monomers long, which provides a compromise between computational efficiency and a chain length representative of the model system. We then use relative entropy minimization to determine the bonded and nonbonded interaction parameters in the CG model (Figure 2b). A staged approach was used for the coarse graining, where parameters determined in a given stage were fixed during subsequent stages. In the first stage, we determined parameters for neat dodecane. For the next stage, we simultaneously coarse grained pBA and pDDA oligomer solutions to

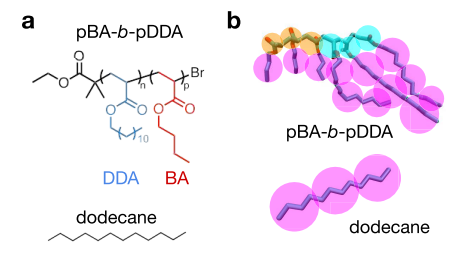


Figure 2. (a) Model system of pBA-*b*-pDDA in a dodecane solvent. (b) CG mapping for the model system. A 3-bead chain represents CG dodecane whereby 4 atomistic carbons are mapped to each of the beads. The same bead type is used to represent the alkyl tails of the acrylic monomers where 1 bead is used for the BA tail and 3 beads for the DDA tail. The acrylate groups are represented by unique bead types for each acrylic species.

determine oligomer self-interactions and oligomer-solvent interactions. Lastly, we coarse grained a solution containing a pBA and pDDA oligomer blend to determine cross interactions between BA and DDA. This type of staged approach suggests a general, practical strategy for the determination of coarse-grained parameters in highly multicomponent systems. For the second and third stages, we used a method previously developed by our group where we impose external potentials to force density inhomogeneities that maximize the number of contacts between CG bead species, which results in concentration- and composition-transferable CG models. More details on the coarse graining procedure and the resulting interaction parameters can be found in Section S2 in the Supporting Information.

After mathematically transforming the fully parametrized CG model into a field-theoretic representation, we evaluate the field theory by invoking a mean-field approximation, called self-consistent field theory (SCFT). 44,67 In SCFT, field fluctuations are ignored and the model is represented by a single dominant field configuration, found by holding the Hamiltonian stationary with respect to variations in the auxiliary fields that define the theory. While the mean-field approximation is most accurate for high molecular weight polymers and dense systems, SCFT has been used to successfully study and characterize phenomena at a variety of length scales, such as phase behavior in block copolymer melts, ^{67,68} colloidal interactions, ⁶⁹ and supramolecular ^{70–72} and surfactant ^{55,73,74} self-assembly. One advantage of the mean-field approach is that the SCFT equations can be solved using a variety of analytical and numerical methods. In particular, the quasi-analytical random phase approximation (RPA)^{50,75} is a computationally inexpensive way to map spinodal boundaries, delineating regions in which a disordered homogeneous phase becomes unstable with respect to macrophase or microphase separation. 44,76 More details on the RPA and its derivation can be found in Section S3.5 in the Supporting Information.

Using RPA analysis, we calculated spinodal boundaries for pBA-b-pDDA in dodecane with a fixed degree of polymerization, N=150, as a function of the diblock copolymer composition, $x_{\rm BA}$ (the mole fraction of BA in the copolymer), and the volume fraction of pBA-b-pDDA in solution, $\phi_{\rm p}$ (Figure 3). The computed spinodals show two U-shaped branches: the first occurs at lower $\phi_{\rm p}$ and higher $x_{\rm BA}$ and terminates at $x_{\rm BA}=1$, which corresponds to the pBA homopolymer limit. Because the copolymers in the region

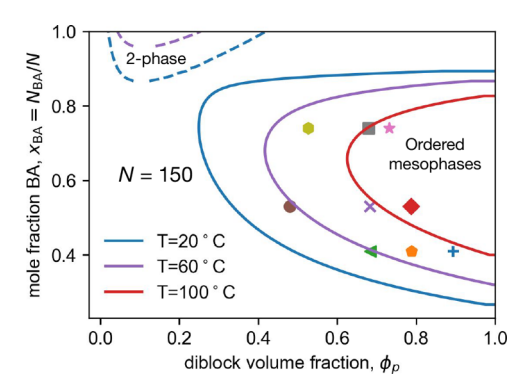


Figure 3. Spinodal boundaries computed using RPA analysis for a pBA-*b*-pDDA diblock copolymer in dodecane with a total degree of polymerization, *N*, of 150. Dashed lines enclose regions of macrophase separation and solid lines regions where ordered mesophases are expected to form, with colors denoting the temperature as indicated in the legend. The symbols correspond to the SAXS spectra from Figure 4.

enveloped by this branch are almost entirely composed of BA, they behave like pBA homopolymers and phase separate into two homogeneous phases, where one phase is more dilute and the other more concentrated in copolymer. This behavior is caused by the solvent-phobic nature of BA at low temperature, which promotes phase separation into polymer-rich domains to limit energetically unfavorable contacts between BA and the dodecane solvent. The size of this two-phase region decreases with temperature and disappears altogether at 100 °C, consistent with the typical increase in solvent quality with temperature. The size of the solvent quality with temperature.

In contrast to the first spinodal envelope, the second occurs at higher ϕ_p and extends to the melt limit at $\phi_p = 1$, enclosing a region where the pBA-b-pDDA copolymers have a more symmetric composition. Here, chemical immiscibility between the pBA and pDDA blocks and solvent selectivity effects drive segregation of the two blocks into domains with widths on the order of the copolymer coil size. These domains order into periodic mesophases that can take on a variety of geometries; we discuss the energetics and stabilities of these structures shortly.

RPA analysis allows us to quickly assess the overall topology of a phase diagram, informing synthetic efforts on specific copolymer lengths and compositions to target. From Figure 3, it is apparent that the predicted ordered mesophase region is centered in the composition range $x_{\rm BA} = 0.4$ to $x_{\rm BA} = 0.8$. Based on this prediction, we used photo-ATRP to synthesize three low-dispersity pBA-*b*-pDDA diblock copolymers that spanned

this composition range and performed SAXS measurements to characterize their solution morphology as functions of concentration and temperature (Figure 4, remaining SAXS spectra in Section S6 in the Supporting Information). Details of the synthesis and characterization procedures are found in Section S5 in the Supporting Information. As highlighted through the many higher-order reflections in the measured spectra, the SAXS results show clear evidence of ordered mesophase formation in the RPA-predicted region, which corroborates the underlying CG model developed for the system. While RPA analysis is unable to provide any information regarding specific morphologies, which we explore using SCFT in subsequent analyses, its ability to quickly elucidate the overall topology of a phase diagram makes it a valuable screening tool for candidate formulations. Crucially, such a rapid tool for accelerating the mapping of phase diagrams is not available in the particle representation of the same CG model.

Experimental Validation of Theory. Subsequent to analytically computing spinodal boundaries, we numerically solve the SCFT equations to probe the formation of spatially inhomogeneous structures. The self-assembly of pBA-*b*-pDDA in these structures is driven by chemical immiscibility and solvent selectivity differences between the two blocks. This causes the pBA and pDDA blocks to segregate into distinct domains to form mesophase structures, and at sufficiently high copolymer concentrations, these domains can order onto periodic lattices. Depending on the relative lengths of the blocks in the copolymer, the mesophases can assume a variety of geometries, such as lamellar, cylindrical, and spherical.

As field-theoretic methods allow ready access to the free energies of different candidate structures, it is straightforward to determine the mesophase that is most thermodynamically favorable (i.e., has the lowest intensive free energy) at any solution conditions. We consider lamellar (LAM), hexagonal (HEX), body-centered cubic (BCC), face-centered cubic (FCC), and double gyroid (GYR) mesophases (Figure 5a), which have been commonly observed in block copolymer solutions. 79-82 Using SCFT, we compute the free energy of each of these structures for all of the as-synthesized pBA-bpDDA diblock copolymers, as functions of both ϕ_p and temperature (Figure 5b). These calculations are performed in conjunction with a variable-cell method that further minimizes the free energy density f with respect to the cell size.⁴⁸ More details are found in Section S3.4 in the Supporting Information.

The results of the SCFT calculations are summarized in the phase diagrams in Figure 6. From Figure 6a, we see excellent agreement between SCFT and SAXS for pBA-b-pDDA with

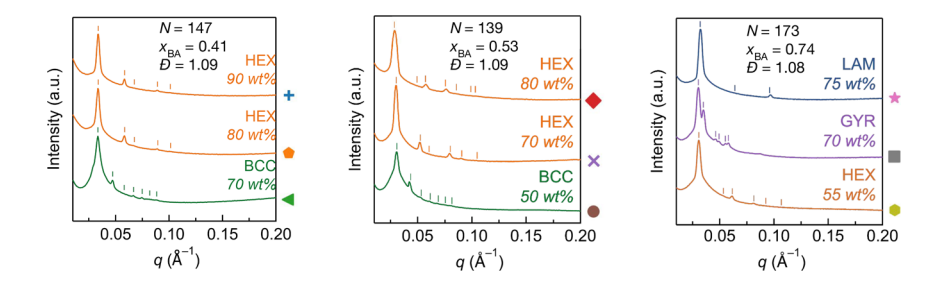


Figure 4. Select SAXS spectra taken at room temperature for the synthesized copolymers at different concentrations. The symbols correspond to the ones in Figure 3 and indicate the position of the spectra relative to the RPA-predicted spinodal boundaries. All additional spectra are found in Section S6 in the Supporting Information.

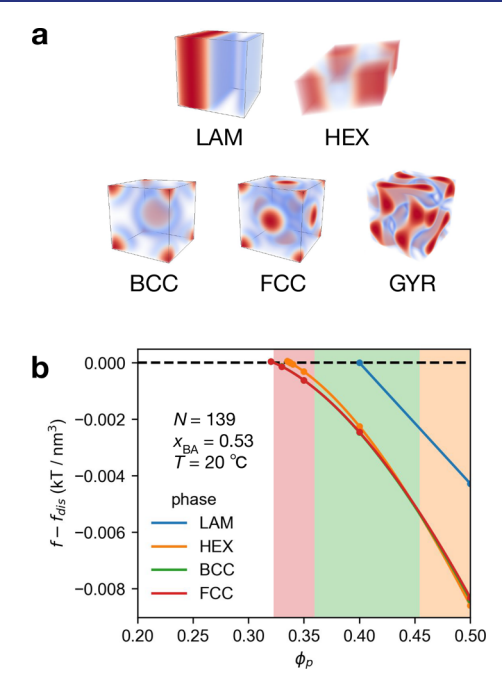
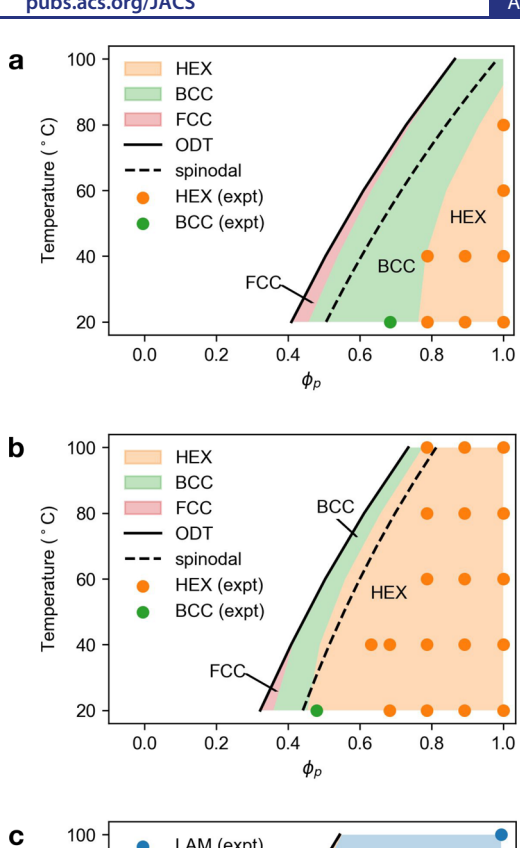


Figure 5. (a) SCFT analysis considers lamellar (LAM), hexagonal (HEX), body-centered cubic (BCC), face-centered cubic (FCC), and double gyroid (GYR) structures. (b) Direct access of SCFT to the free energy density f enables the determination of the most favorable morphology at each set of conditions, as that which minimizes f. Shown is the free energy of each candidate structure relative to that for the homogeneous, disordered phase at the same conditions.

the shortest pBA block ($x_{BA} = 0.41$). Specifically, the theoretical prediction quantitatively locates the BCC to HEX transition with increasing ϕ and the shifting of the order– disorder transition (ODT) to higher $\phi_{
m p}$ with increasing temperature. At lower $\phi_{
m p}$, spherical structures are stabilized when the dodecane solvent selectively enters and swells the pDDA regions, stretching the corona and favoring structures with larger interfacial curvature. At increased ϕ_p , this solventinduced swelling is minimized so that structures with less interfacial curvature, such as cylinders, are favored. For the pBA-*b*-pDDA copolymer with $x_{BA} = 0.53$ (Figure 6b), we again see excellent agreement between SCFT and SAXS where the BCC to HEX transition is quantitatively predicted. One main difference between this phase diagram and the previous one is the presence of a larger HEX region. This shift is caused by the relatively larger pBA block, which increases the size of the core and increases the amount of solvent necessary to sufficiently swell the corona to form spherical structures.

The final pBA-b-pDDA copolymer with $x_{BA} = 0.74$ has a richer phase behavior than the previous two copolymers (Figure 6c). This allowed us to examine all classical morphologies including LAM, HEX, BCC, FCC, and GYR, and demonstrate agreement between de novo theory and experiment. In the phase diagram for this final copolymer (Figure 6c), the large LAM region is caused by the relatively large pBA block which favors structures with minimal interfacial curvature. Additionally, the narrow GYR window captured using both computation and experiment demonstrates the ability of the field theory to inform the synthesis of formulations targeting phases with small windows of stability that would be otherwise easily missed. While SCFT is able to capture the experimentally observed HEX to GYR to LAM phase transitions, the phase boundaries are shifted to lower $\phi_{\rm p}$



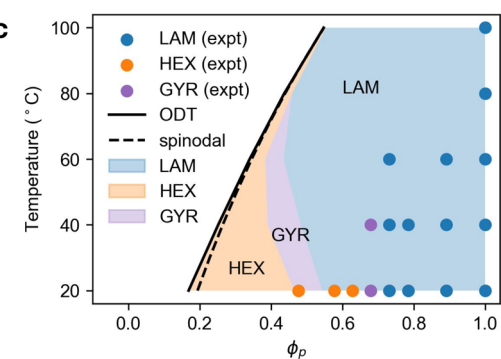


Figure 6. Temperature-vs-concentration phase diagrams for pBA-bpDDA copolymers with N = 147, $x_{BA} = 0.41$, and D = 1.09 (a), N =139, $x_{BA} = 0.53$, and D = 1.09 (b), and N = 173, $x_{BA} = 0.74$, and D = 1.091.08 (c). The shaded regions indicate SCFT predictions of stable phases while the dots indicate experimentally observed mesophases from SAXS measurements. The solid black line indicates the ODT while the dashed black line indicates the spinodal boundary.

in the computational predictions. One possible explanation for the discrepancy between theory and experiment in this case is that the training of the CG model was performed on systems with compositional symmetry ($x_{BA} = 0.5$), which is much closer to the composition of the other two samples. Another potential explanation is that the $x_{BA} = 0.74$ copolymer has nearly overlapping spinodal and order-disorder transition (ODT) curves across much of the ODT boundary, suggesting that the phase transition is very weakly first-order. Under such conditions, field fluctuations are known to be very strong, stabilizing the disordered phase relative to ordered phases. Consequently, our use of SCFT, which invokes the mean-field approximation, under-predicts $\phi_{\rm p}$ at the ODT. While this shortcoming can be remedied by employing more computationally expensive fully fluctuating FTS, 46 which should bring the experimental and computational results in closer agreement, the use of a mean-field approximation does not significantly hinder the ability of our framework to anticipate phase behavior across a broad range of compositions, concentrations, and temperatures.

CONCLUSIONS

We have developed a multiscale workflow to produce molecularly informed field-theoretic models that accurately predict mesoscale properties of polymer formulations without the need for any experimental input. This framework was used to parametrize field-theoretic models for pBA-b-pDDA diblock copolymers in dodecane solvent, and we applied the models to target specific copolymer compositions for synthesis and SAXS analysis. Significantly, the field-theoretic models were found to quantitatively predict mesophase formation as functions of temperature, concentration, and diblock composition for the as-synthesized, well-defined samples. The ability to perform mesoscale simulations while retaining connections to underlying atomic-scale chemistry enables efficient in silico prediction of properties for complex, multicomponent systems. This is expected to accelerate the development of formulations with new and sustainable chemistries. Future work will focus on extending the capabilities of this workflow through the directed synthesis of libraries of functional block copolymers. This combination of simulation and synthesis will enable the calculation of other properties of interest, such as critical micelle concentrations under more dilute conditions, and the development of methods to predict interfacial properties and self-assembly behavior near surfaces.

ASSOCIATED CONTENT

5 Supporting Information

The Supporting Information is available free of charge at https://pubs.acs.org/doi/10.1021/jacs.4c11258.

Atomistic simulation details, coarse graining procedure, CG force field details, particle-to-field transformation, details on SCFT calculations and RPA analysis, experimental procedures, and SAXS spectra (PDF)

AUTHOR INFORMATION

Corresponding Authors

Craig J. Hawker — Materials Research Laboratory,
Department of Chemistry and Biochemistry, Materials
Department, and Mitsubishi Chemical Center for Advanced
Materials, University of California, Santa Barbara, Santa
Barbara, California 93106, United States; occid.org/
0000-0001-9951-851X; Email: hawker@mrl.ucsb.edu

M. Scott Shell — Department of Chemical Engineering and Mitsubishi Chemical Center for Advanced Materials, University of California, Santa Barbara, Santa Barbara, California 93106, United States; ⊚ orcid.org/0000-0002-0439-1534; Email: shell@engineering.ucsb.edu

Glenn H. Fredrickson — Department of Chemical Engineering, Materials Research Laboratory, Materials Department, and Mitsubishi Chemical Center for Advanced Materials, University of California, Santa Barbara, Santa Barbara, California 93106, United States; orcid.org/0000-0002-6716-9017; Email: ghf@mrl.ucsb.edu

Authors

Charles Li — Department of Chemical Engineering, University of California, Santa Barbara, Santa Barbara, California 93106, United States; orcid.org/0000-0003-0788-7233

Elizabeth A. Murphy — Materials Research Laboratory and Department of Chemistry and Biochemistry, University of California, Santa Barbara, Santa Barbara, California 93106, United States; orcid.org/0000-0003-0846-7943

Stephen J. Skala — Materials Research Laboratory and Materials Department, University of California, Santa Barbara, Santa Barbara, California 93106, United States Kris T. Delaney — Materials Research Laboratory, University of California, Santa Barbara, Santa Barbara, California 93106, United States; orcid.org/0000-0003-0356-1391

Complete contact information is available at: https://pubs.acs.org/10.1021/jacs.4c11258

Notes

The authors declare the following competing financial interest(s): This work was financially supported by the Mitsubishi Chemical Corporation (MCC). Glenn H. Fredrickson is a member of the Board of Directors of the Mitsubishi Chemical Group, the parent company of MCC.

ACKNOWLEDGMENTS

This work was supported by Mitsubishi Chemical Corporation (MCC) through the Mitsubishi Chemical Center for Advanced Materials and by the BioPACIFIC Materials Innovation Platform of the National Science Foundation under award no. DMR-1933487. Use was made of computational facilities purchased with funds from the National Science Foundation (CNS-1725797, OAC-1925717) and administered by the Center for Scientific Computing (CSC). The CSC is supported by the California NanoSystems Institute and the Materials Research Science and Engineering Center (MRSEC; NSF DMR 2308708) at UC Santa Barbara. C.L., E.A.M., and S.J.S. gratefully acknowledge the NSF Graduate Research Fellowship Program (GRFP) under grant no. 2139319.

REFERENCES

- (1) Kataoka, K.; Harada, A.; Nagasaki, Y. Block copolymer micelles for drug delivery: design, characterization and biological significance. *Adv. Drug Delivery Rev.* **2001**, *47*, 113–131.
- (2) Yang, J. Viscoelastic wormlike micelles and their applications. Curr. Opin. Colloid Interface Sci. 2002, 7, 276–281.
- (3) Dreiss, C. A. Wormlike micelles: where do we stand? Recent developments, linear rheology and scattering techniques. *Soft Matter* **2007**, *3*, 956–970.
- (4) Zheng, R.; Liu, G.; Devlin, M.; Hux, K.; Jao, T.-C. Friction Reduction of Lubricant Base Oil by Micelles and Crosslinked Micelles of Block Copolymers. *Tribiol. Trans.* **2009**, *53*, 97–107.
- (5) Fielding, L. A.; Lane, J. A.; Derry, M. J.; Mykhaylyk, O. O.; Armes, S. P. Thermo-responsive Diblock Copolymer Worm Gels in Non-polar Solvents. *J. Am. Chem. Soc.* **2014**, *136*, 5790–5798.
- (6) Derry, M. J.; Fielding, L. A.; Armes, S. P. Industrially-relevant polymerization-induced self-assembly formulations in non-polar solvents: RAFT dispersion polymerization of benzyl methacrylate. *Polym. Chem.* **2015**, *6*, 3054–3062.
- (7) Derry, M. J.; Fielding, L. A.; Warren, N. J.; Mable, C. J.; Smith, A. J.; Mykhaylyk, O. O.; Armes, S. P. In situ small-angle X-ray scattering studies of sterically-stabilized diblock copolymer nanoparticles formed during polymerization-induced self-assembly in nonpolar media. *Chemical Science* **2016**, *7*, 5078–5090.

- (8) Derry, M. J.; Mykhaylyk, O. O.; Armes, S. P. A Vesicle-to-Worm Transition Provides a New High-Temperature Oil Thickening Mechanism. *Angew. Chem.* **2017**, *129*, 1772–1776.
- (9) Danov, K. D.; Kralchevsky, P. A.; Stoyanov, S. D.; Cook, J. L.; Stott, I. P.; Pelan, E. G. Growth of wormlike micelles in nonionic surfactant solutions: Quantitative theory vs. experiment. *Adv. Colloid Interface Sci.* **2018**, 256, 1–22.
- (10) Davies, A.; Amin, S. Microstructure design of CTAC:FA and BTAC:FA lamellar gels for optimized rheological performance utilizing automated formulation platform. *Int. J. Cosmet. Sci.* **2020**, 42, 259–269.
- (11) Chandrasegaran, S. K.; Ramani, K.; Sriram, R. D.; Horváth, I.; Bernard, A.; Harik, R. F.; Gao, W. The evolution, challenges, and future of knowledge representation in product design systems. *Computer-Aided Design* **2013**, *45*, 204–228.
- (12) Cao, L.; Russo, D.; Lapkin, A. A. Automated robotic platforms in design and development of formulations. *AIChE J.* **2021**, *67*, No. e17248.
- (13) Delidovich, I.; Hausoul, P. J. C.; Deng, L.; Pfützenreuter, R.; Rose, M.; Palkovits, R. Alternative Monomers Based on Lignocellulose and Their Use for Polymer Production. *Chem. Rev.* **2016**, *116*, 1540–1599.
- (14) Zhu, Y.; Romain, C.; Williams, C. K. Sustainable polymers from renewable resources. *Nature* **2016**, *540*, 354–362.
- (15) Hillmyer, M. A. The promise of plastics from plants. *Science* **2017**, 358, 868–870.
- (16) Hong, M.; Chen, E. Y. X. Future Directions for Sustainable Polymers. *Trends in Chemistry* **2019**, *1*, 148–151.
- (17) Li, T.; Chen, C.; Brozena, A. H.; Zhu, J. Y.; Xu, L.; Driemeier, C.; Dai, J.; Rojas, O. J.; Isogai, A.; Wågberg, L.; Hu, L. Developing fibrillated cellulose as a sustainable technological material. *Nature* **2021**, *590*, 47–56.
- (18) Cywar, R. M.; Rorrer, N. A.; Hoyt, C. B.; Beckham, G. T.; Chen, E. Y.-X. Bio-based polymers with performance-advantaged properties. *Nat. Rev. Mater.* **2022**, *7*, 83–103.
- (19) Gartner, T. E.; Jayaraman, A. Modeling and Simulations of Polymers: A Roadmap. *Macromolecules* **2019**, *52*, 755–786.
- (20) Lee, O.-S.; Stupp, S. I.; Schatz, G. C. Atomistic Molecular Dynamics Simulations of Peptide Amphiphile Self-Assembly into Cylindrical Nanofibers. *J. Am. Chem. Soc.* **2011**, *133*, 3677–3683.
- (21) Tang, X.; Koenig, P. H.; Larson, R. G. Molecular Dynamics Simulations of Sodium Dodecyl Sulfate Micelles in Water—The Effect of the Force Field. *J. Phys. Chem. B* **2014**, *118*, 3864–3880.
- (22) Ramasamy, U. S.; Lichter, S.; Martini, A. Effect of Molecular-Scale Features on the Polymer Coil Size of Model Viscosity Index Improvers. *Tribol Lett.* **2016**, *62*, 23.
- (23) Ramasamy, U. S.; Len, M.; Martini, A. Correlating Molecular Structure to the Behavior of Linear Styrene–Butadiene Viscosity Modifiers. *Tribol. Lett.* **2017**, *65*, 147.
- (24) Gupta, J.; Nunes, C.; Vyas, S.; Jonnalagadda, S. Prediction of Solubility Parameters and Miscibility of Pharmaceutical Compounds by Molecular Dynamics Simulations. *J. Phys. Chem. B* **2011**, *115*, 2014–2023.
- (25) Wojnarowska, Z.; Grzybowska, K.; Hawelek, L.; Dulski, M.; Wrzalik, R.; Gruszka, I.; Paluch, M.; Pienkowska, K.; Sawicki, W.; Bujak, P.; Paluch, K. J.; Tajber, L.; Markowski, J. Molecular Dynamics, Physical Stability and Solubility Advantage from Amorphous Indapamide Drug. *Mol. Pharmaceutics* **2013**, *10*, 3612–3627.
- (26) Müller-Plathe, F. Coarse-Graining in Polymer Simulation: From the Atomistic to the Mesoscopic Scale and Back. *ChemPhysChem* **2002**, *3*, 754–769.
- (27) Morita, H.; Tanaka, K.; Kajiyama, T.; Nishi, T.; Doi, M. Study of the Glass Transition Temperature of Polymer Surface by Coarse-Grained Molecular Dynamics Simulation. *Macromolecules* **2006**, 39, 6233–6237.
- (28) Karimi-Varzaneh, H. A.; van der Vegt, N. F. A.; Müller-Plathe, F.; Carbone, P. How Good Are Coarse-Grained Polymer Models? A Comparison for Atactic Polystyrene. *ChemPhysChem* **2012**, *13*, 3428–3439.

- (29) Hall, K. W.; Sirk, T. W.; Klein, M. L.; Shinoda, W. A coarse-grain model for entangled polyethylene melts and polyethylene crystallization. *J. Chem. Phys.* **2019**, *150*, 244901.
- (30) Albina, J.-M.; Kubo, A.; Shiihara, Y.; Umeno, Y. Coarse-Grained Molecular Dynamics Simulations of Boundary Lubrication on Nanostructured Metal Surfaces. *Tribol. Lett.* **2020**, *68*, 49.
- (31) Dhamankar, S.; Webb, M. A. Chemically specific coarse-graining of polymers: Methods and prospects. *J. Polym. Sci.* **2021**, *59*, 2613–2643.
- (32) Fang, Y.; Yue, T.; Li, S.; Zhang, Z.; Liu, J.; Zhang, L. Molecular Dynamics Simulations of Self-Healing Topological Copolymers with a Comblike Structure. *Macromolecules* **2021**, *54*, 1095–1105.
- (33) Joshi, S. Y.; Deshmukh, S. A. A review of advancements in coarse-grained molecular dynamics simulations. *Mol. Simul.* **2021**, 47, 786–803.
- (34) Shen, K.-H.; Fan, M.; Hall, L. M. Molecular Dynamics Simulations of Ion-Containing Polymers Using Generic Coarse-Grained Models. *Macromolecules* **2021**, *54*, 2031–2052.
- (35) Coldstream, J. G.; Camp, P. J.; Phillips, D. J.; Dowding, J. P. Gradient copolymers versus block copolymers: self-assembly in solution and surface adsorption. *Soft Matter* **2022**, *18*, 6538–6549.
- (36) Hoogerbrugge, P. J.; Koelman, J. M. V. A. Simulating Microscopic Hydrodynamic Phenomena with Dissipative Particle Dynamics. *EPL* **1992**, *19*, 155.
- (37) Koelman, J. M. V. A.; Hoogerbrugge, P. J. Dynamic Simulations of Hard-Sphere Suspensions Under Steady Shear. *EPL* **1993**, *21*, 363.
- (38) Español, P.; Warren, P. Statistical Mechanics of Dissipative Particle Dynamics. EPL 1995, 30, 191.
- (39) Groot, R. D.; Warren, P. B. Dissipative particle dynamics: Bridging the gap between atomistic and mesoscopic simulation. *J. Chem. Phys.* **1997**, *107*, 4423–4435.
- (40) Weiß, H.; Deglmann, P.; in't Veld, P. J.; Cetinkaya, M.; Schreiner, E. Multiscale Materials Modeling in an Industrial Environment. *Annu. Rev. Chem. Biomol. Eng.* **2016**, *7*, 65–86.
- (41) Saathoff, J. Effectively parameterizing dissipative particle dynamics using COSMO-SAC: A partition coefficient study. *J. Chem. Phys.* **2018**, *148*, 154102.
- (42) Santo, K. P.; Neimark, A. V. Dissipative particle dynamics simulations in colloid and Interface science: a review. *Adv. Colloid Interface Sci.* **2021**, 298, No. 102545.
- (43) Willner, L.; Poppe, A.; Allgaier, J.; Monkenbusch, M.; Richter, D. Time-resolved SANS for the determination of unimer exchange kinetics in block copolymer micelles. *EPL* **2001**, *55*, 667.
- (44) Fredrickson, G. The Equilibrium Theory of Inhomogeneous Polymers; Oxford University Press: 2006.
- (45) Liu, Y.-X.; Delaney, K. T.; Fredrickson, G. H. Field-Theoretic Simulations of Fluctuation-Stabilized Aperiodic "Bricks-and-Mortar" Mesophase in Miktoarm Star Block Copolymer/Homopolymer Blends. *Macromolecules* **2017**, *50*, 6263–6272.
- (46) Fredrickson, G. H.; Delaney, K. T. Field-Theoretic Simulations in Soft Matter and Quantum Fluids; Oxford University Press: 2023.
- (47) Lequieu, J. Combining particle and field-theoretic polymer models with multi-representation simulations. *J. Chem. Phys.* **2023**, 158, 244902.
- (48) Barrat, J.-L.; Fredrickson, G. H.; Sides, S. W. Introducing Variable Cell Shape Methods in Field Theory Simulations of Polymers. *J. Phys. Chem. B* **2005**, *109*, 6694–6700.
- (49) Fredrickson, G. H.; Delaney, K. T. Direct free energy evaluation of classical and quantum many-body systems via field-theoretic simulation. *Proc. Natl. Acad. Sci. U. S. A.* **2022**, *119*, No. e2201804119.
- (50) Gennes, P.-G. D. Scaling Concepts in Polymer Physics; Cornell University Press: 1979.
- (51) Willis, J. D.; Beardsley, T. M.; Matsen, M. W. Simple and Accurate Calibration of the Flory–Huggins Interaction Parameter. *Macromolecules* **2020**, *53*, 9973–9982.
- (52) Sherck, N.; Shen, K.; Nguyen, M.; Yoo, B.; Köhler, S.; Speros, J. C.; Delaney, K. T.; Shell, M. S.; Fredrickson, G. H. Molecularly Informed Field Theories from Bottom-up Coarse-Graining. *ACS Macro Lett.* **2021**, *10*, 576–583.

- (53) Nguyen, M.; Sherck, N.; Shen, K.; Edwards, C. E. R.; Yoo, B.; Köhler, S.; Speros, J. C.; Helgeson, M. E.; Delaney, K. T.; Shell, M. S.; Fredrickson, G. H. Predicting Polyelectrolyte Coacervation from a Molecularly Informed Field-Theoretic Model. *Macromolecules* **2022**, *55*, 9868–9879.
- (54) Shen, K.; Nguyen, M.; Sherck, N.; Yoo, B.; Köhler, S.; Speros, J.; Delaney, K. T.; Shell, M. S.; Fredrickson, G. H. Predicting surfactant phase behavior with a molecularly informed field theory. *J. Colloid Interface Sci.* **2023**, *638*, 84–98.
- (55) Nguyen, M.; Shen, K.; Sherck, N.; Köhler, S.; Gupta, R.; Delaney, K. T.; Shell, M. S.; Fredrickson, G. H. A molecularly informed field-theoretic study of the complexation of polycation PDADMA with mixed micelles of sodium dodecyl sulfate and ethoxylated surfactants. *Eur. Phys. J. E* **2023**, *46*, 75.
- (56) Honda, K.; Morita, M.; Otsuka, H.; Takahara, A. Molecular Aggregation Structure and Surface Properties of Poly(fluoroalkyl acrylate) Thin Films. *Macromolecules* **2005**, 38, 5699–5705.
- (57) Li, T.; Li, H.; Wang, H.; Lu, W.; Osa, M.; Wang, Y.; Mays, J.; Hong, K. Chain flexibility and glass transition temperatures of poly(nalkyl (meth)acrylate)s: Implications of tacticity and chain dynamics. *Polymer* **2021**, *213*, No. 123207.
- (58) Shell, M. S. The relative entropy is fundamental to multiscale and inverse thermodynamic problems. *J. Chem. Phys.* **2008**, *129*, 144108.
- (59) Shell, M. S. Coarse-graining with the relative entropy. *Advances in chemical physics* **2016**, *161*, 395–441.
- (60) Carmichael, S. P.; Shell, M. S. A New Multiscale Algorithm and Its Application to Coarse-Grained Peptide Models for Self-Assembly. *J. Phys. Chem. B* **2012**, *116*, 8383–8393.
- (61) Carmichael, S. P.; Shell, M. S. Entropic (de)stabilization of surface-bound peptides conjugated with polymers. *J. Chem. Phys.* **2015**, *143*, 243103.
- (62) Sanyal, T.; Mittal, J.; Shell, M. S. A hybrid, bottom-up, structurally accurate, Gō-like coarse-grained protein model. *J. Chem. Phys.* **2019**, *151*, No. 044111.
- (63) Pretti, E.; Shell, M. S. Mapping the configurational landscape and aggregation phase behavior of the tau protein fragment PHF6. *Proc. Natl. Acad. Sci. U. S. A.* **2023**, *120*, No. e2309995120.
- (64) Shen, K.; Sherck, N.; Nguyen, M.; Yoo, B.; Köhler, S.; Speros, J.; Delaney, K. T.; Fredrickson, G. H.; Shell, M. S. Learning composition-transferable coarse-grained models: Designing external potential ensembles to maximize thermodynamic information. *J. Chem. Phys.* **2020**, *153*, 154116.
- (65) Stratonovich, R. On a method of calculating quantum distribution functions. Sov. Phys. Dokl. 1957, 2, 416-419.
- (66) Hubbard, J. Calculation of Partition Functions. *Phys. Rev. Lett.* **1959**, 3, 77–78.
- (67) Arora, A.; Qin, J.; Morse, D. C.; Delaney, K. T.; Fredrickson, G. H.; Bates, F. S.; Dorfman, K. D. Broadly Accessible Self-Consistent Field Theory for Block Polymer Materials Discovery. *Macromolecules* **2016**, *49*, 4675–4690.
- (68) Matsen, M. W. Field theoretic approach for block polymer melts: SCFT and FTS. J. Chem. Phys. 2020, 152, 110901.
- (69) Li, W.; Delaney, K. T.; Fredrickson, G. H. Self-consistent field theory study of polymer mediated colloidal interactions in solution: Depletion effects and induced forces. *J. Chem. Phys.* **2021**, *155*, 154903.
- (70) Feng, E. H.; Lee, W. B.; Fredrickson, G. H. Supramolecular Diblock Copolymers: A Field-Theoretic Model and Mean-Field Solution. *Macromolecules* **2007**, *40*, 693–702.
- (71) Lee, W. B.; Elliott, R.; Katsov, K.; Fredrickson, G. H. Phase Morphologies in Reversibly Bonding Supramolecular Triblock Copolymer Blends. *Macromolecules* **2007**, *40*, 8445–8454.
- (72) Fredrickson, G. H.; Delaney, K. T. Coherent states field theory in supramolecular polymer physics. *J. Chem. Phys.* **2018**, *148*, 204904.
- (73) Thompson, R. B.; Jebb, T.; Wen, Y. Benchmarking a self-consistent field theory for small amphiphilic molecules. *Soft Matter* **2012**, *8*, 9877–9885.

- (74) Ginzburg, V. V. Mesoscale Modeling of Micellization and Adsorption of Surfactants and Surfactant-Like Polymers in Solution: Challenges and Opportunities. *Ind. Eng. Chem. Res.* **2022**, *61*, 15473—15487.
- (75) Gennes, P.-G. D. Some conformation problems for long macromolecules. *Rep. Prog. Phys.* **1969**, *32*, 187–205.
- (76) Leibler, L. Theory of Microphase Separation in Block Copolymers. *Macromolecules* **1980**, *13*, 1602–1617.
- (77) Hanley, K. J.; Lodge, T. P.; Huang, C.-I. Phase Behavior of a Block Copolymer in Solvents of Varying Selectivity. *Macromolecules* **2000**, 33, 5918–5931.
- (78) Ianiro, A.; Hendrix, M. M.; Hurst, P. J.; Patterson, J. P.; Vis, M.; Sztucki, M.; Esteves, A. C. C.; Tuinier, R. Solvent Selectivity Governs the Emergence of Temperature Responsiveness in Block Copolymer Self-Assembly. *Macromolecules* **2021**, *54*, 2912–2920.
- (79) Shibayama, M.; Hashimoto, T.; Kawai, H. Ordered structure in block polymer solutions. 1. Selective solvents. *Macromolecules* **1983**, *16*, 16.
- (80) Wanka, G.; Hoffmann, H.; Ulbricht, W. Phase Diagrams and Aggregation Behavior of Poly(oxyethylene)-Poly(oxypropylene)-Poly(oxyethylene) Triblock Copolymers in Aqueous Solutions. *Macromolecules* 1994, 27, 4145.
- (81) Lodge, T. P.; Bang, J.; Park, M. J.; Char, K. Origin of the thermoreversible fcc-bcc transition in block copolymer solutions. *Physical review letters* **2004**, 92, No. 145501.
- (82) Lodge, T. P.; Pudil, B.; Hanley, K. J. The Full Phase Behavior for Block Copolymers in Solvents of Varying Selectivity. *Macromolecules* **2002**, *35*, 4707–4717.
- (83) Fredrickson, G. H.; Helfand, E. Fluctuation effects in the theory of microphase separation in block copolymers. *J. Chem. Phys.* **1987**, 87, 697–705.